41 Combustion of Lean Mixtures Initiated by an Imploding Detonation Plug

Kazuro HOTTA[1], Tatsuaki INOUE[1], Osamu MORIUE[1],
Teruo TATEFUKU[2], Minoru SUZUKI[2], and Eiichi MURASE[1]
Kyushu University[1], JFE Engineering Co.[2]

744 Motooka, Nishi-ku, Fukuoka 819-0395, Japan

In spark ignition engines, lean burn and high compression ratio operation are effective to minimize NOx emission and maximize the thermal efficiency. However, lean burn often leads to problems such as low ignition probability and low burning rate, and high compression ratio operation often leads to knocking. In order to prevent them, an Imploding Detonation (ID) plug is a quite attractive ignition device producing high energy plasma jet by the active use of imploding detonation. In this study, fundamental characteristics of the combustion and the lean limit in the combustion chamber initiated by the ID plug were investigated by OH fluorescence measurements based on Planner Laser Induced Fluorescence (PLIF) and pressure measurements.

Key words: **Engine combustion/ Spark ignition engines, Imploding detonation, Planner laser induced fluorescence**

1. INTRODUCTION

In spark ignition engines, lean burn and high compression ratio operation are effective to minimize NOx emission and maximize the thermal efficiency. However, lean burn often leads to problems such as low ignition probability and low burning rate, and high compression ratio operation often leads to knocking. The technique of Pulsed Flame Jet (PFJ) ignition is one of the most prospective ways to prevent these problems [1-4]. The concept of PFJ ignition is to provide a number of ignition kernels widely across the combustion chamber by injection of active radicals. It was reported that sufficiently high burning rate and ignition probability in the combustion of lean mixtures are achieved by PFJ [1-4].

Presented here is another type of a unique jet ignition by the active use of imploding detonation. The high energy plasma jet produced by the Imploding Detonation (ID) plug spreads in the combustion chamber significantly faster. In this study, fundamental characteristics of the combustion and the lean limit in the combustion chamber initiated by the ID plug were investigated by the combustion tests in the constant volume combustion chamber. The diagnostic methods used were OH fluorescence measurements based on Planer Laser Induced Fluorescence (PLIF) and pressure measurements.

2. EXPERIMENTAL SETUP

2.1 IMPLODING DETONATION (ID) PLUG

The ID plug shown in Fig. 1 consists of a precombustion chamber, a converging chamber, a separating valve, and an exit nozzle. When the separating valve was opened, the fuel/air mixture charged in the precombustion chamber was ignited by an ordinary spark plug at an atmospheric pressure and a room temperature. Then an imploding detonation was induced in the conversing chamber, and a high energy plasma jet was issued from the exit nozzle into the combustion chamber.

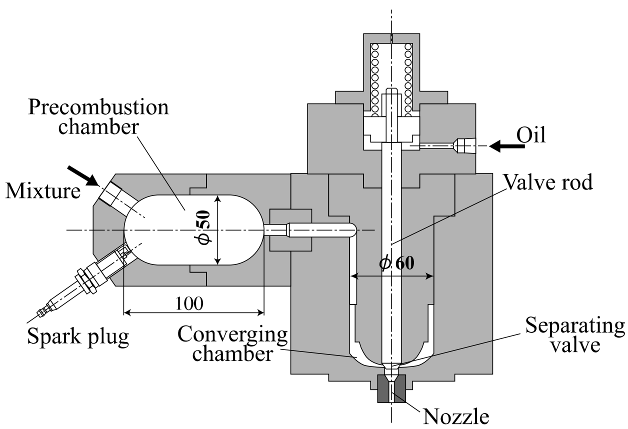

Fig. 1 Imploding Detonation (ID) plug

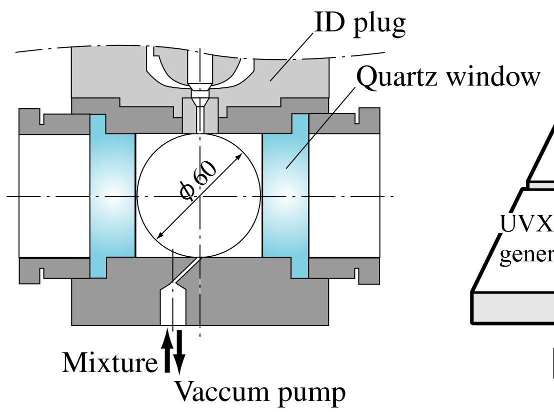

Fig. 2 Combustion chamber

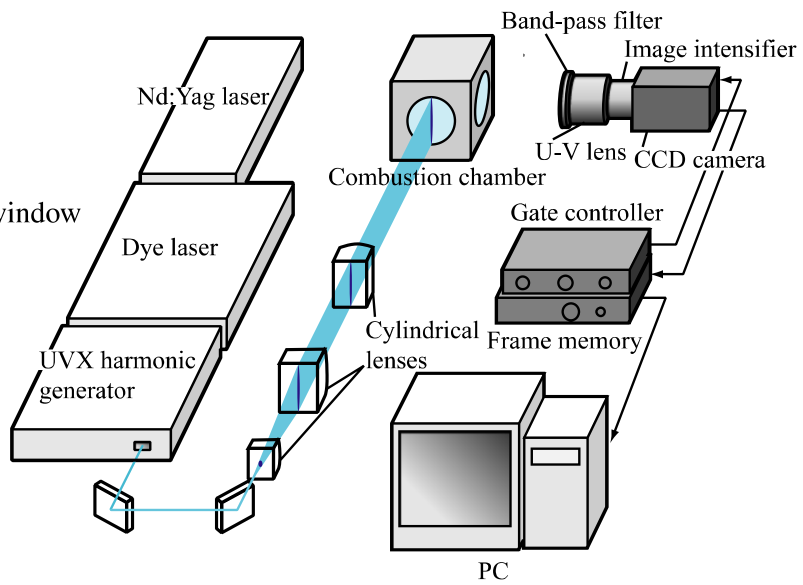

Fig. 3 Schematic diagram of PLIF system

Table 1 Specifications of lasers

Nd:YAG laser	: Continuum Surelite Ⅲ-10
Pulse energy	: 800 mJ/pulse at 1064 nm
Pulse width	: 4 ns ~ 6 ns
Dye laser	: Continuum ND6000 with UVX harmonic generator
Dye	: Rhodamine 590

Table 2 Specifications of ICCD camera

Image intensifier	: Delft Electronische Produkten Type XX1450CK
Spectral sensitivity	: 193 nm ~ 780 nm
Gate width	: 25 ns ~ 33 ms
CCD camera	: SONY XC-77
CCD pixels	: 768 × 493
Lens	: UV-Nikkor 105 mm *f*/4.5

In this study, the mixture used was methane/air and the equivalence ratio of the mixture in the ID plug was unity. In order to induce imploding detonation under the circumstance of an atmospheric pressure and a room temperature, oxygen enriched air were used. Here, the oxygen concentration was defined as the volume percentage of the oxygen in the oxygen enriched air.

2.2 COMBUSTION CHAMBER

The combustion chamber used is shown in Fig. 2. It was consisted of two cylinders of 60 mm in diameter, joined together in the middle. Four quartz glass windows were equipped on the both opposite ends. The ID plug was attached to the top of the chamber, and the pressure transducer was installed on the bottom of the chamber.

2.3 LASER SYSTEM

The experimental setup for OH fluorescence measurement is depicted schematically in Fig. 3. The system consists of a tunable pulsed dye laser (Continuum ND6000) pumped by a Nd:YAG laser (Continuum Surelite III -10), and a wavelength extension package (Continuum UVX harmonic generator) which is a frequency doubling unit using a KDP crystal. Then, OH was pumped at the X $^2\Pi$ (ν = 1) – A $^2\Sigma$ (ν = 0) transition at 283 nm, and the fluorescence from the A $^2\Sigma$ (ν = 0) – X $^2\Pi$ (ν = 0) transition was collected [3, 4, 6]. The height and the thickness of the laser sheet were about 60 mm and 0.5 mm, respectively. The fluorescence from the excited OH was collected with a UV lens and a band-pass filter (central wavelength: 307.8 nm, half width: 14.1 nm, maximum transmissivity: 20.5%), and it was imaged by the time-gated ICCD camera. In order to eliminate OH emission at 306.4 nm, the gate width of the ICCD camera used was set to 100 ns. A single-shot OH image was once stored on a frame memory, and then it was transmitted to a personal computer for processing. Note that the OH fluorescence images provided in this paper are nonconsecutive, i.e., each image was acquired from a different combustion test. The timing of the events, such as the single-shot Nd:YAG laser operation, the ICCD camera operation, and the starting of the spark discharge etc., was controlled by a computer.

3. RESULTS AND DISCUSSION

3.1 EFFECTS OF NOZZLE DIAMETER

In the investigation of the PFJ ignition (1-4), the action of the jet strongly depended on the orifice diameter of the PFJ igniter. Thus, in this study, three different nozzle diameters of the ID plug, D = 2, 3, and 4 mm were investigated. The oxygen concentration in the ID plug and the equivalence ratio in the combustion chamber were fixed at 34 % and 0.83, respectively.

Typical examples of the OH fluorescence images and the measured pressure profiles in the combustion chamber initiated by the ID plug are displayed with time after the ignition in the ID plug, τ, in Figs. 4 and 5, respectively. The delay time in the initiation of the pressure rise was observed in Fig. 5, which can be considered to be the induction time of the imploding detonation. The rate of pressure rise and the maximum pressure were increased by the use of the large nozzle diameter. In Fig. 4, the diameter of the region viewed was 60 mm, and the degree of brightness of the images corresponds to the OH fluorescence intensity. As the induction time of the imploding detonation existed, the OH fluorescence in the combustion chamber was observed at τ = 6.85 ms. The intense OH fluorescence was observed in the whole fluorescence area, which is the evidence of the volumetric combustion initiated by the ID plug. Compared with PFJ (1-4), the penetration of the jet issued from the ID plug was significantly faster and deeper. Since the flow was choked at the exit of the nozzle, the momentum of the jet was increased by the use of the large nozzle diameter. Thus, the penetration depth of the jet increased with the increase of the nozzle diameter, D. The impingements of the jet on the wall, which are concerned to cause both momentum and heat losses, were observed, and the time of the impingement became shorter with the increase of the nozzle diameter, D.

In order to quantify the effects of the nozzle diameter, the variations of OH fluorescence area, its mean intensity, and the

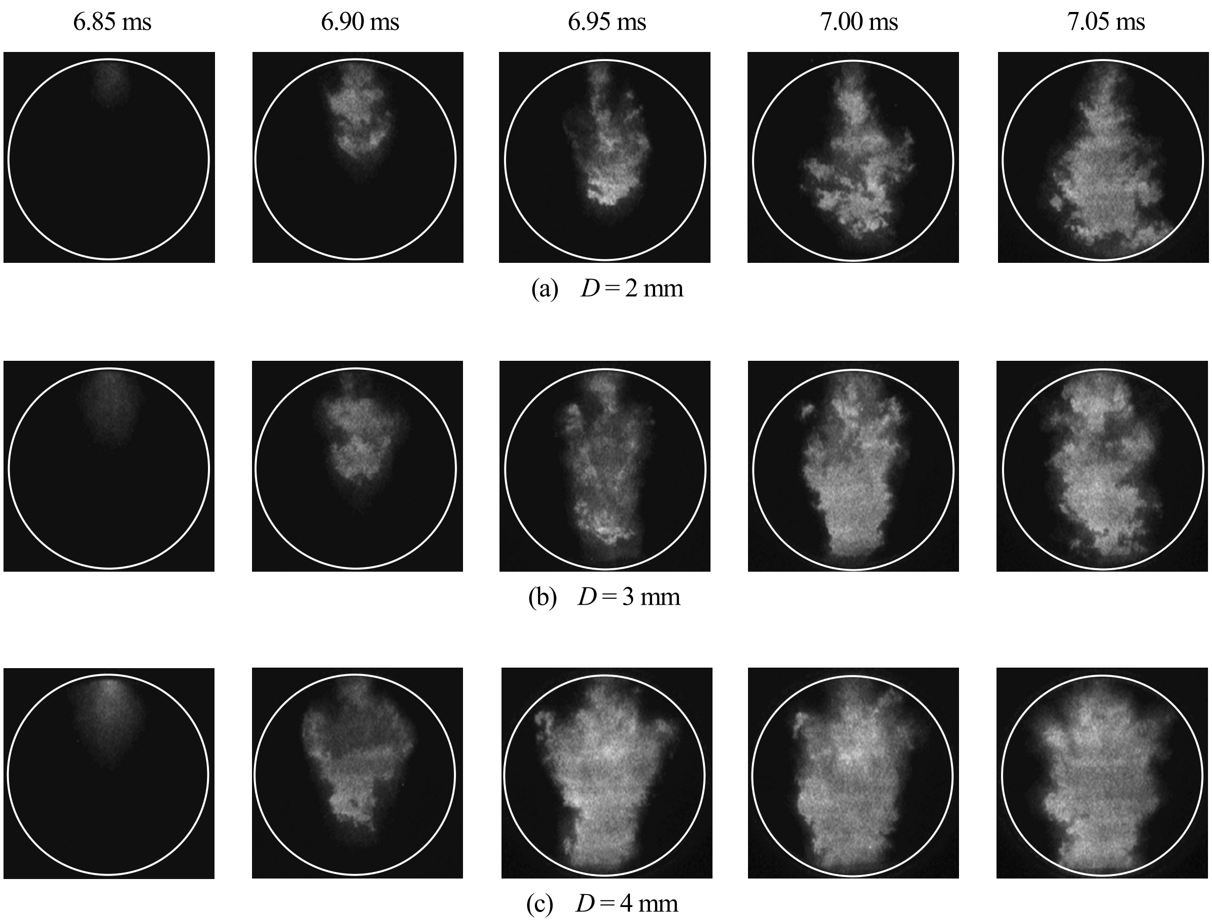

Fig. 4 OH fluorescence images of combustion initiated by ID plug

total intensity with time after the ignition in the ID plug, τ, are depicted in Figs. 6, 7, and 8, respectively. Here, the mean intensity was defined by the intensity averaged in the whole fluorescence area, and the total intensity was defined by the intensity integrated over the whole fluorescence area. The OH fluorescence area presented in Fig. 6 increased monotonously with time, τ, and it was increased by the use of the large nozzle diameter.

Here, the entrainment degree of the unburned mixture into the jet was thought to be the main factor of the development of the OH fluorescence area. Thus, the volume of a nonreactive turbulent jet was evaluated as shown in the following discussion, and it was compared to the measured OH fluorescence volume which is given by the 3/2 power of the OH fluorescence area.

A theoretical circular turbulent jet is assumed [7], thus

$$V \propto x^3 \qquad (1)$$

where, V denotes the volume of the jet, and x denotes the distance from the virtual origin of the jet.

While, according to a dimensional analysis on the circular turbulent jet [7],

$$\frac{u_x}{u_0} \propto \frac{D}{x} \qquad (2)$$

where, u_x and u_0 denote the flow velocity at $x = x$, and at the exit of the nozzle, respectively. Assuming that u_0 is the same (the sound velocity) in each nozzle diameter, D;

$$u_x = \frac{dx}{d\tau} \propto \frac{D}{x} \qquad (3)$$

The integration of Eq. (3) gives

$$\int_0^x x dx \propto D \int_{\tau_0}^{\tau} d\tau$$

$$\therefore \quad x \propto \sqrt{D\left(\tau - \tau_0\right)} \qquad (4)$$

where, τ_0 denotes the time of the beginning of the jet issued from the nozzle. Eqs. (1) and (4) yield,

$$V \propto \left\{D\left(\tau - \tau_0\right)\right\}^{3/2} \qquad (5)$$

Thus, in order to compare the measured OH fluorescence volume and the volume of the nonreactive circular turbulent jet described by Eq. (5), the following equation is derived.

$$\alpha = \left\{\frac{OH\ fluorecence\, area}{D\left(\tau - \tau_0\right)}\right\}^{3/2} \qquad (6)$$

According to Fig. 4, the time $\tau_0 = 6.80$ was assumed, and then the variation of α with time, τ, is presented in Fig. 9. During the beginning of the combustion, the large value of α was attained with larger nozzle diameter, that is, the volume of the OH fluorescence was effectively increased by the chemical reaction initiated by the active species contained in the jet. Thus, the enhancement of the ignition probability can be expected by the use of the large nozzle diameter. The values of α increased till the jet impinged to the opposed wall, and then decreased. This decrease of α was considered to be caused by both momentum and heat losses occurred by the impingement of the jet on the wall. As the time of the impingement became shorter with the increase of the nozzle diameter, D, as shown in Fig. 4, the peak of α became earlier with the increase of the nozzle diameter, D.

As shown in Fig. 7, the difference in the mean OH fluorescence intensity depending on the nozzle diameter, D, was relatively small. Thus, the tendency of the total OH fluorescence intensity shown in Fig. 8 was similar to that of the OH fluorescence area shown in Fig. 6.

The lean limit in the combustion chamber was investigated and the results are summarized in Table 3. The oxygen concentration in the ID plug was fixed at 34 %. From Table 3, the lean limit was extended with the increase of the nozzle diameter, D.

3.2 EFFECTS OF OXYGEN ENRICHMENT

The effects of the oxygen enrichment in the ID plug were investigated. Figure 10 presents the measured pressure profiles of the combustion initiated by the ID plug of 30-36% oxygen concentration. The nozzle diameter, D, and the equivalent ratio in the combustion chamber, ϕ, were fixed at 3 mm and 0.83, respectively. Since the burning rate was enhanced by the oxygen enrichment, the induction time of the imploding detonation was reduced by the increase of oxygen enrichment. Thus, the delay time in the initiation of the pressure rise in the combustion chamber was reduced with increasing in the oxygen enrichment in the ID plug. Although the adiabatic temperature, the pressure, and the burning rate are theoretically increased by oxygen enrichment, the rate of pressure rise and the maximum pressure shown in Fig. 10 were decreased. The reason of this result can be considered that the momentum of the jet was increased by the oxygen enrichment, and it caused the larger impingement of the jet on the wall.

Table 4 shows the ignition probability in the different oxygen enrichment and the different nozzle diameter, D. The equivalence ratio in the combustion chamber was 0.83. The ignition probability was increased with the increase in the oxygen enrichment in the ID plug in each nozzle diameter, D.

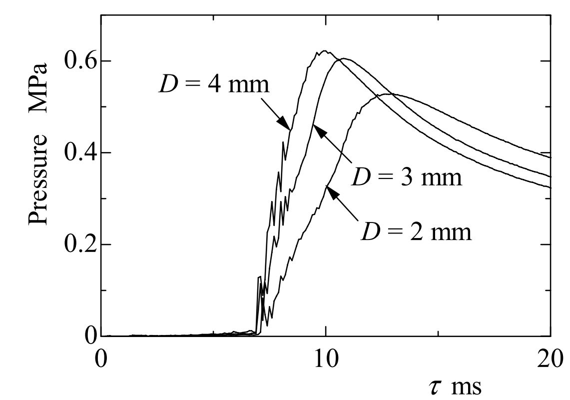

Fig. 5 Measured pressure profiles in the different nozzle diameter (ϕ = 0.83, ϕ_{ID} = 1.0, Oxygen concentration 34 %)

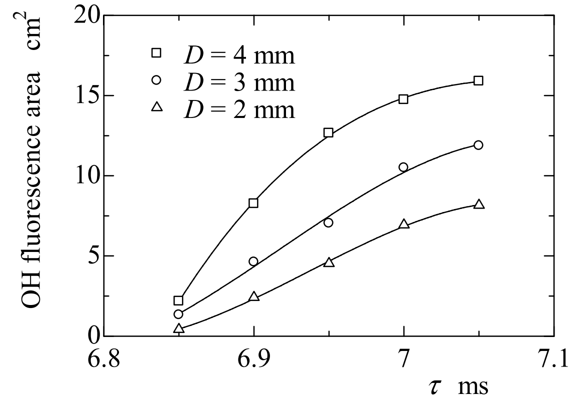

Fig. 6 Variation of OH fluorescence area after the ignition in ID plug (ϕ = 0.83, ϕ_{ID} = 1.0, Oxygen concentration 34 %)

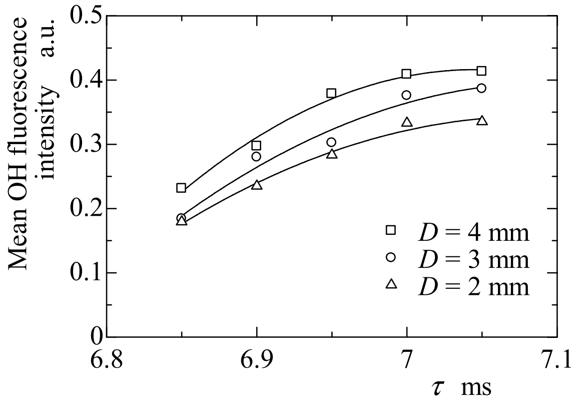

Fig. 7 Variation of mean OH fluorescence intensity after the ignition in ID plug (ϕ = 0.83, ϕ_{ID} = 1.0, Oxygen concentration 34 %)

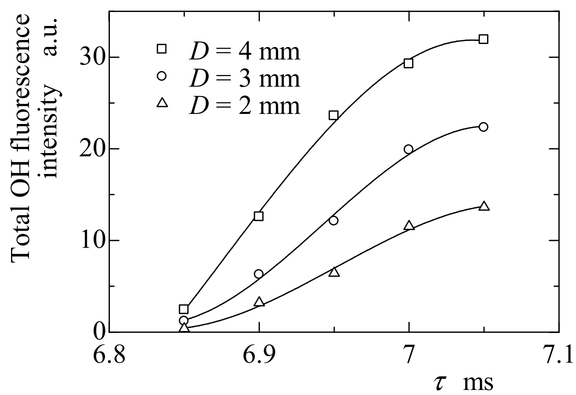

Fig. 8 Variation of total OH fluorescence intensity after the ignition in ID plug (ϕ = 0.83, ϕ_{ID} = 1.0, Oxygen concentration 34 %)

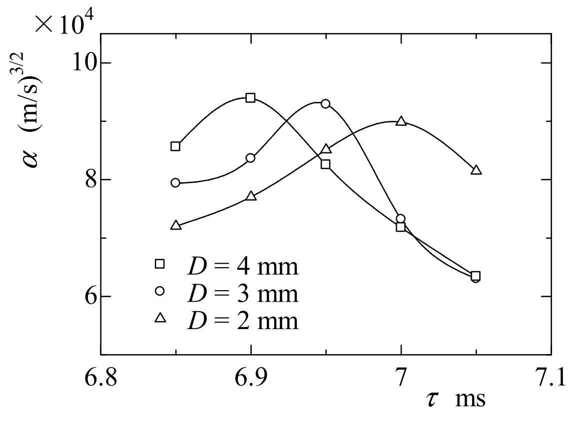

Fig. 9 Variation of α after the ignition in ID plug (ϕ = 0.83, ϕ_{ID} = 1.0, Oxygen concentration 34 %)

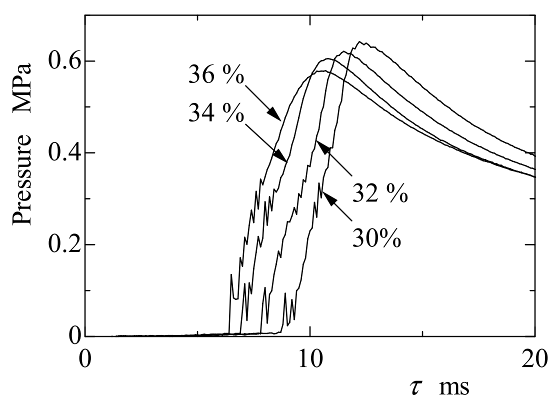

Fig. 10 Measured pressure profiles in the different oxygen concentration (ϕ = 0.83, D = 3 mm, ϕ_{ID} = 1.0)

Table 3 Lean limit in the different nozzle diameters (Oxygen concentration 34 %)

D (mm) \ ϕ	0.77	0.71	0.67	0.63	0.59	0.56	0.53	0.50	0.48	0.45	0.43	0.42	0.40
2	○	○	●	●	●	●	●	●	●	●	●	●	●
3	○	○	○	○	○	○	●	●	●	●	●	●	●
4	○	○	○	○	○	○	○	○	○	○	○	○	●

○ Burned, ● Unburned

Table 4 Ignition probability in the different oxygen enrichment and nozzle diameters (ϕ= 0.83)

D (mm) \ O_2 (vol%)	34	33	32	31	30	29	28
2	100%	75%	75%	50%	0%	0%	0%
3	100%	100%	100%	100%	100%	0%	0%
4	100%	100%	100%	100%	100%	100%	0%

4. CONCLUSIONS

(1) The penetration of the jet issued in the combustion chamber from the ID plug was significantly faster and deeper, compared with the PFJ. Thus, rapid combustion process and high ignition reliability were obtained by the use of the ID plug.

(2) The effects of the nozzle diameter of the ID plug were investigated. The combustion was enhanced, and lean limit in the combustion chamber was extended by the use of the large nozzle diameter. However, the increase of the nozzle diameter leaded both momentum and heat losses of the jet caused by its impingement on the wall. Thus, the use of optimally designed multiple nozzles, each of which is preventing the impingement of the jet on the wall, will improve the ignition probability and the enhancement of the combustion.

(3) The oxygen enrichment in the ID plug reduced the induction time of the imploding detonation, concomitantly increased the ignition probability in each nozzle diameter.

5. REFERENCES

(1) Murase, E., Ono, S., Hanada, K., and Oppenheim, A.K., A Comparative Study of Pulsed Jet Ignition, JSAE Review, 13, No. 2, pp. 19-23, 1992.

(2) Murase, E., Ono, S., Hanada, K., and Oppenheim, A.K., Initiation of Combustion in Lean Mixtures by Flame Jets, Combust. Sci. and Tech., Vols. 113-114, pp.167-177, 1996.

(3) Murase, E. and Hanada, K., Enhancement of Combustion by Injection of Radicals, SAE Trans., Journal of Engines, 109, Sec. 3, pp. 34-41, 2001.

(4) Murase, E., Hanada, K., T. Hamakawa, T., and Hotta, K, Effects of Spark Discharge Mode in Pulsed Flame Jet Igniter on OH Fluorescence Images in a Swirl Flow, Combust. Sci. and Tech., Vol. 176, pp.1639-1652, 2004.

(5) Eckbreth, A.C., Bonczyk, P.A., and Verdieck, J.F., Combustion Diagnostics by Laser Raman and Fluorescence Techniques, Progress in Energy and Combustion Science, 5, pp. 253-322, 1979.

(6) Hanson, R.K., Combustion Diagnostics: Planar Imaging Techniques, Proceedings of the Combustion Institute, 21, pp.1677-1691, 1986.

(7) Rajaratnum, N., Turbulent jets, Elsevier Scientific, 1976.